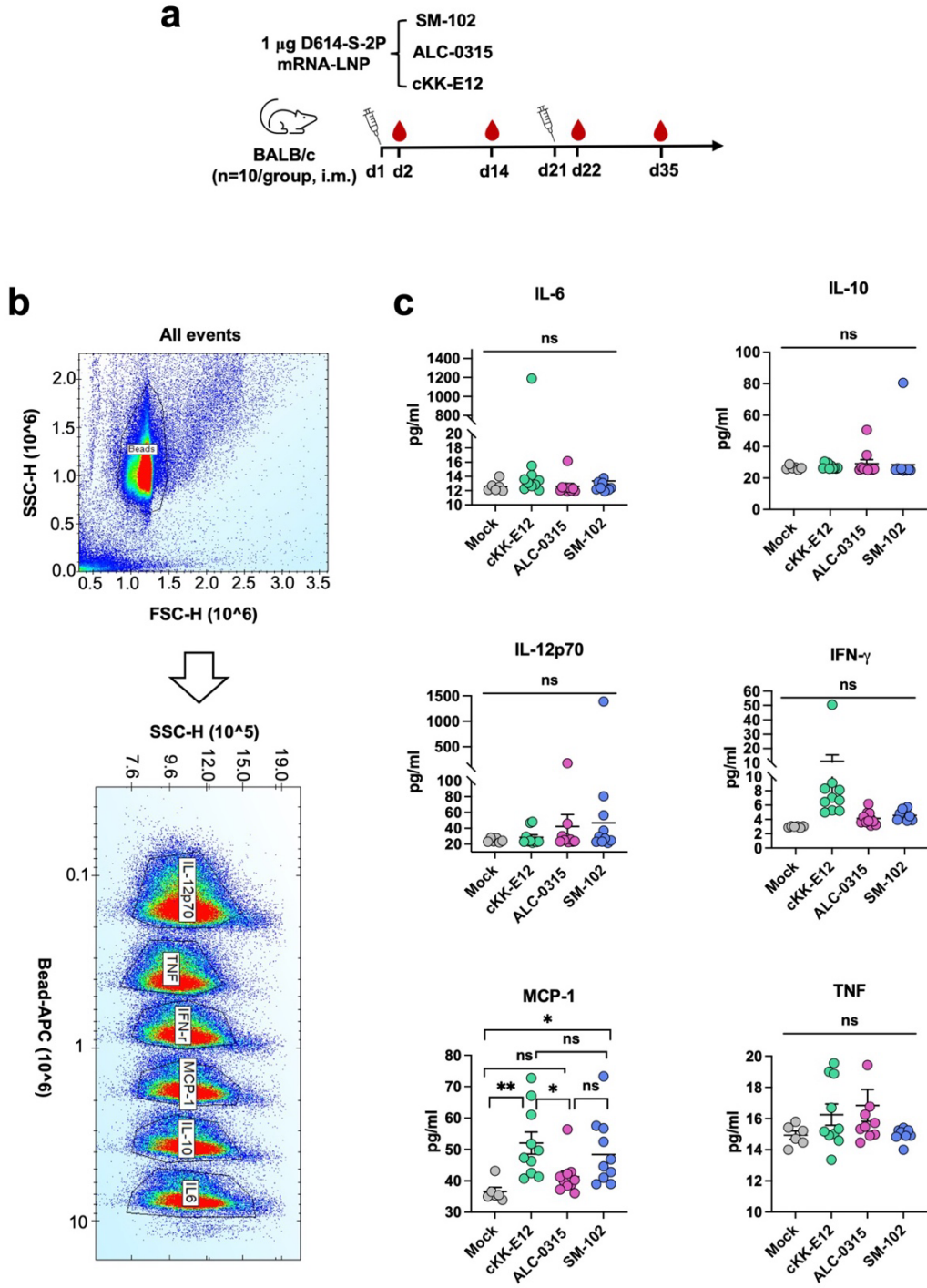
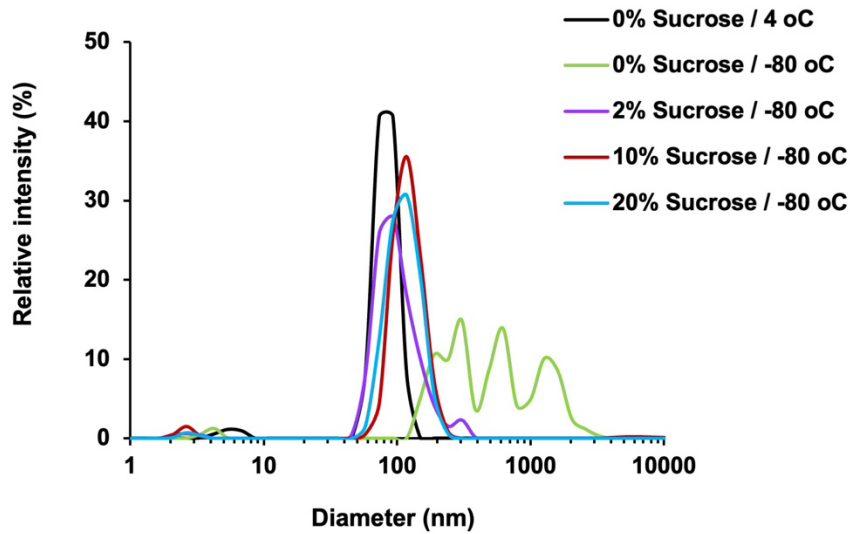


Supplementary Materials



Supplementary Figure 1. (Related to Fig. 2). SM-102 and ALC-0315 LNP inflammatory responses compared to cKK-E12 LNP one day after a boost immunization. **a** Timeline of mouse immunization and bleeding. Ten BALB/c mice per group were intramuscularly vaccinated at the indicated days, each time with 1 μ g SARS-CoV-2 spike mRNA-LNP prepared with the indicated ionizable lipid. Blood was collected at the indicated time points to measure cytokines and neutralizing antibodies. **b** Gating strategy of the flowcytometry for both d2 and d22 cytokines/chemokines detection. Within the cytokines/chemokines population, PE fluorescence intensity was measured to reflect the amount of bound cytokines/chemokines. **c** Pro-inflammatory cytokines/chemokines in the d22 plasma were measured using the murine inflammation kit and analyzed by Accuri Flow cytometer. Data are presented as Mean \pm SEM of n = 10 mice per group. Statistical significance among the groups was analyzed by one-way ANOVA with Tukey's multiple comparisons test (ns, not significant; * p < 0.05, ** p < 0.01).



Supplementary Figure 2. (Related to Fig. 3). Effect of sucrose on mRNA-LNP size and storage at -80 °C. Size distribution of LNP was measured by DLS; mRNA-LNP was supplied with varying amount of sucrose and kept either at 4 °C or at -80 °C. LNP size was measured after thawing for those frozen at -80 °C. Sucrose protects LNP from aggregation during freeze-and-thawing. Sucrose effect on LNP size increase is observed only between 2 and 10%.

a

Pfizer/BioNTech 5'UTR:

GAGAATAAAGTAGTATTCTTCTGGTCCCCACAGACTCAGAGAGAACCCGCCACC

Pfizer/BioNTech 3'UTR:

CTCGAGCTGGTACTGCATGCACGCAATGCTAGCTGCCCTTTCCGGTCTGGGTACCCCGAGTCTCCCCGGACC
TCGGGTCCCAGGTATGCTCCACCTCCACCTGCCCCACTCACCACCTCTGCTAGTTCCAGACACCTCCAAGCA
CGCAGCAATGCAGCTCAAAACGCTTAGCCTAGCCACACCCCCACGGGAAACAGCAGTGATTAACCTTTAGCAATA
AACGAAAGTTTAACTAAGCTATACTAACCCAGGGTTGGTCAATTTCTGTGCCAGCCACACCTGGAGCTAGC

Moderna 5'UTR:

GGGAAATAAGAGAGAAAAGAAGAGTAAGAAGAAATATAAGACCCCGGCGCCGCCACC

Moderna 3'UTR:

GCTGGAGCCTCGGTGGCCTAGCTTCTTGCCCTTGGGCCTCCCCCAGCCCTCCTCCCCTTCTGCACCCGTA
CCCCGTGGTCTTTGAATAAAGTCTGAGTGGGCGGCA

TEV 5'UTR:

TCTCAACACAACATATACAAAACAAACGAATCTCAAGCAATCAAGCATTCTACTTCTATTGCAGCAATTTAAATCAT
TTCTTTTAAAGCAAAAGCAATTTTCTGAAAATTTTACCATTACGAACGATAGC

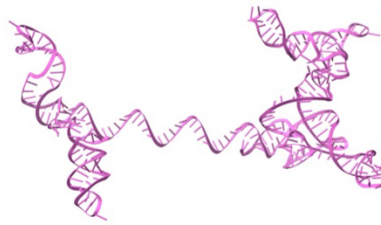
TEV 3'UTR:

AGTGACTGACTAGGATCTGGTTACCACTAAACCAGCCTCAAGAACACCCGAATGGAGTCTCTAAGCTACATAATA
CCAACTTACACTTACAAAATGTTGTCCCCAAAATGTAGCCATTGATCTGCTCCTAATAAAAAGAAAGTTTCTTC
ACATTCT

b



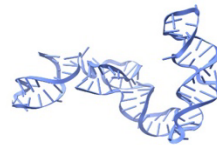
Pfizer/BioNTech 5'UTR
 $\Delta G = -9.20$ kcal/mol



Pfizer/BioNTech 3'UTR
 $\Delta G = -91.20$ kcal/mol



Moderna 5'UTR
 $\Delta G = -3.24$ kcal/mol



Moderna 3'UTR
 $\Delta G = -33.50$ kcal/mol



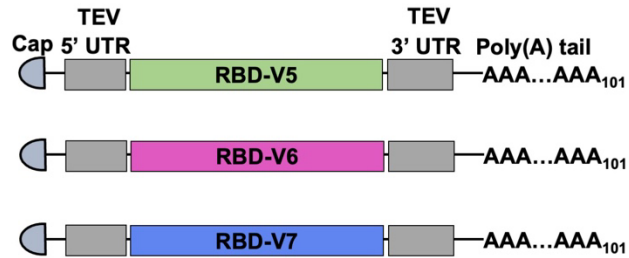
TEV 5'UTR
 $\Delta G = -8.60$ kcal/mol



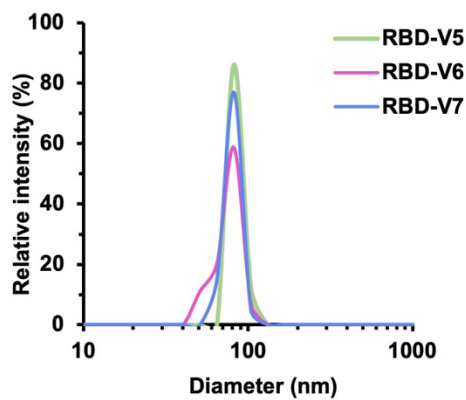
TEV 3'UTR
 $\Delta G = -26.10$ kcal/mol

Supplementary Figure 3. (Related to Fig. 5) The sequences and secondary structures of the UTRs from the Pfizer/BioNTech and Moderna COVID-19 vaccines. a 5' and 3' UTR sequences. TEV is our own vector for *in vitro* transcription. The Kozak sequence is underlined and the high GC tract immediately upstream of the Kozak sequence in Moderna's 5' UTR is italicized. **b** RNA secondary structures were predicted by M-fold (<http://www.unafold.org/mfold/applications/rna-folding-form.php>), and their 3D structures were modelled using RNA Composer (<https://macomposer.cs.put.poznan.pl/>).

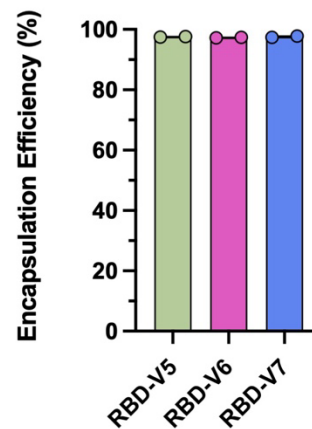
a



b



c



Supplementary Figure 4. (Related to Fig. 6) Particle size and encapsulation efficiency of RBD mRNA-LNPs with varying m¹Ψ content. a Schematic diagrams of the RBD mRNAs used in the study with varying wobble m¹Ψ content but with the same 5' cap, UTRs, and poly(A) tail. **b** Size distribution of RBD mRNA-LNPs in 10% sucrose was measured by DLS. **c** Encapsulation efficiency of these LNPs was measured by the Quant-it™ RiboGreen RNA Assay Kit.